



Published in final edited form as:

Anal Chem. 2012 April 17; 84(8): 3795–3801. doi:10.1021/ac300468a.

Electrothermal Supercharging of Proteins in Native Electrospray Ionization

Harry J. Sterling, Catherine A. Cassou, Anna C. Susa, and Evan R. Williams*

Department of Chemistry, University of California, Berkeley, California 94720-1460

Abstract

The formation of high charge-state protein ions with nanoelectrospray ionization (nESI) from purely aqueous ammonium bicarbonate solutions at neutral pH, where the proteins have native or native-like conformations prior to ESI droplet formation, is demonstrated. This “electrothermal” supercharging method depends on the temperature of the instrument entrance capillary, the nESI spray potential, and the solution ionic strength and buffer, although other factors almost certainly contribute. Mass spectra obtained with electrothermal supercharging appear similar to those obtained from denaturing solutions where charging beyond the total number of basic sites can be achieved. For example, a 17+ ion of bovine ubiquitin was formed by nESI of a 100 mM ammonium bicarbonate, pH 7.0, solution, which is three more charges than the total number of basic amino acids plus the N-terminus. Heating of the ESI droplets in the vacuum/atmosphere interface, and the concomitant denaturation of the protein *in the ESI droplets* prior to ion formation, appears to be the primary origin of the very high charge-state ions formed from these purely aqueous, buffered solutions. nESI mass spectra resembling those obtained under traditional native or denaturing conditions can be reversibly obtained simply by toggling the spray voltage between low and high values.

Introduction

With electrospray ionization (ESI), proteins, DNA, macromolecular complexes, and even intact viruses can be readily ionized from purely aqueous or buffered aqueous solutions, a method often referred to as “native” mass spectrometry.¹ The solution-phase properties of macromolecules can be probed, including binding affinities,² changes in protein conformation,³ the stoichiometries of protein complexes,^{4–6} or protein complex assembly kinetics and thermodynamics.^{7,8} Charge-state distributions of proteins and protein complexes from native solutions tend to be narrow and centered at high m/z . For example, the charge-state distribution for intact 3.0 MDa Hepatitis B virus capsids is centered around the 133+ charge-state at m/z 22,500.⁹ Time-of-flight mass spectrometers are typically used to analyze such large complexes because of the more limited m/z ranges of most other types of mass spectrometers.

The formation of ions with high charge is often desirable because the sensitivity and resolution of most mass spectrometers improves at lower m/z , and tandem mass spectrometry (MS/MS) is typically more efficient and structurally informative when higher charge-state ions are produced.^{10–12} This is especially true for electron capture or electron transfer dissociation experiments performed on Fourier-transform ion cyclotron resonance (FT-ICR) or Orbitrap™ mass spectrometers, because both the capture/transfer cross section^{13,14} and ion detection¹⁵ increase substantially with ion charge. High charge-state

*Address reprint requests to Prof. Evan R. Williams: Department of Chemistry, University of California, Berkeley, B42 Hildebrand Hall, Berkeley, CA 94720, Phone: (510) 643-7161, FAX: (510) 642-7714, erw@berkeley.edu.

ions of proteins or other molecules that can change conformational states are commonly formed from “denaturing” solutions that typically contain high concentrations of organic solvents, and/or at extremes of solution pH.^{16,17} The resulting ESI mass spectra generally have broad distributions of high charge-state ions as a result of unfolding the protein in the original solution prior to ion formation.^{18,19} Although the resulting high charge-states are ideal for MS/MS experiments, all native structure and function of the protein is lost in the initial solutions.

An alternative approach to form high charge-state ions is to use supercharging reagents. Originally demonstrated with denaturing solutions,^{20–26} this method also works well for proteins formed from native solutions.^{27–39} A supercharging reagent is added to the ESI solution at low initial concentration, but because these reagents have high boiling points compared to the other solvents, enrichment of the reagent occurs during the ESI droplet evaporation process.^{34,40} Studies of the origin of supercharging from denaturing solutions containing water/methanol/acetic acid indicate that an increase in the solvent surface tension due to reagent enrichment allows for more highly charged ESI droplets and, thus, more charge available for the protein at the time of ion formation,^{20–22} although this mechanism has not been universally accepted.^{41,42} In contrast, supercharging reagents added to aqueous or buffered aqueous solutions can result in chemical and/or thermal denaturation of the protein or protein complex analytes *in the ESI droplets*.^{29–34} Experiments using circular dichroism,^{31,34} HDX-MS,^{33,34} and chemical crosslinking^{30,32} show that the conformations of proteins and protein complexes in the initial solution are unaffected by the low concentration of the supercharging reagent, but unfolding of proteins and/or conformational changes to protein complexes are caused by the increased concentration of these reagents in the ESI droplets, and these conformational changes are the origin of native supercharging.^{29–34}

A key advantage to forming high charge protein ions with supercharging reagents is that the native conformations of the analytes remain undisturbed until ESI droplets are formed.^{30–34} Conformation changes occur during the ms or even sub-ms timescale of the droplet lifetime⁴³ prior to ion formation.^{29–34} However, the supercharging effect is limited by the conformational flexibility and stability of the folded form of the analyte³⁰ and is therefore highly protein-dependent. Some researchers have found that the extent of supercharging with these reagents is insufficient to significantly shift some analyte charge-state distributions to lower m/z where better sensitivity and resolution can be attained.^{44,45}

Here, a supercharging effect that can be controlled by a combination of entrance capillary temperature, ESI spray potential, and the ionic strength of ammonium bicarbonate used to buffer the protein solutions at neutral pH is described. Results from experiments exploring these variables indicate that unfolding of the protein analytes that occurs *in the ESI droplets* is the primary origin of the supercharging effect, and that the effect can be attributed to thermal denaturation that is enhanced by additional protein destabilization due to the presence of the bicarbonate anion. The extent of supercharging from native solutions achieved with this very simple and reversible technique is significantly higher than what can be obtained with supercharging reagents, like *m*-NBA or sulfolane, in native MS.

Experimental

Mass spectra were acquired using either a Thermo LTQ-orbitrap™ or FT-ICR hybrid mass spectrometer (Thermo Fischer Scientific, Waltham, MA, USA), a Waters Q-TOF Premier™ hybrid mass spectrometer (Waters, Milford, MA, USA) or the Berkeley-Bruker 9.4 T FT-ICR mass spectrometer.⁴⁶ Ions were formed using nanoelectrospray emitters prepared by pulling borosilicate capillaries (1.0 mm o.d./0.78 mm i.d., Sutter Instruments, Novato, CA,

USA) to a tip i.d. of $\sim 1 \mu\text{m}$ with a Flaming/Brown micropipette puller (Model P-87, Sutter Instruments, Novato, CA, USA). A platinum wire (0.127 mm diameter, Sigma, St. Louis, MO, USA) was placed in the nanoelectrospray emitter in contact with the solution and 5 mm from the emitter tip. ESI was initiated by applying $\sim 1.0 \text{ kV}$ to the wire relative to the instrument ground with the emitter tip positioned 5 mm from the entrances of the Thermo or Waters instruments, or 3 mm from the entrance of the Berkeley-Bruker instrument. The spray potential was then increased or decreased incrementally for studies of the effects of spray potential on the analyte charge-state distributions, while all other instrument parameters were kept constant. The values for *Fraction Unfolded* are calculated by dividing the sum of the relative abundances for “high-charge” peaks in the protein charge-state distribution by the sum of the relative abundances for all peaks in the protein charge-state distribution. “High-charge” and “low-charge” peaks correspond to the two bell-shaped curves of the observed bimodal distributions. Error bars or precision values are one standard deviation of the mean of the replicate measurements at a given experimental condition. Proteins and ammonium bicarbonate, perchlorate, phosphate and sulfate salts were from Sigma (St. Louis, MO, USA) and used without further purification. Ammonium acetate was from Fischer Scientific (Pittsburgh, PA, USA) and ammonium thiocyanate was from J.T. Baker (Center Valley, PA, USA), and both were used without further purification. Detailed descriptions of the individual experiments are provided in the Supporting Information.

Results and Discussion

Effects of Source Temperature and Spray Potential on Protein Charge-state Distributions

The effects of the temperature of the heated metal entrance capillary (Thermo LTQ) on the charge-state distributions (CSD) obtained from nESI of bovine ubiquitin (20 μM , 200 mM ammonium bicarbonate, pH 7.0, aqueous solution; 1.2 kV spray potential) are shown in Figure 1a-c. At 150 $^{\circ}\text{C}$ (Figure 1c), the CSD is narrow and is dominated by the 5+ charge-state. In contrast, the CSD at 300 $^{\circ}\text{C}$ (Figure 1a) is much broader, and is centered around the 10+ charge-state. At 200 $^{\circ}\text{C}$ (Figure 1b), the CSD is bimodal with distributions centered around both the 5+ and 10+ charge-states. The narrow CSD at low charge-state measured at 150 $^{\circ}\text{C}$ (Figure 1c) is consistent with typical “native” ESI spectra of ubiquitin,^{47,48} and the broad CSD of predominantly high charge ions at 300 $^{\circ}\text{C}$ (Figure 1a) is more consistent with spectra of ubiquitin measured from denaturing conditions.^{49,50} Similar transitions from a narrow, low-charge CSD to a bimodal CSD of low- and high-charge ions, and then to a predominantly high-charge CSD have been observed previously by incremental chemical¹⁷ and thermal⁵¹ denaturation of ubiquitin in the bulk ESI solution. The range of charge-states observed here at 300 $^{\circ}\text{C}$ (17+ – 4+) is broader, with higher maximum charge, than that observed previously by Loo *et al.* for ubiquitin electrosprayed from a denaturing solution of 18:77:5 acetonitrile:water:acetic acid (13+ – 7+)¹⁷ or by Chait and coworkers who heated an unbuffered aqueous ESI solution (pH 2.8) to 93 $^{\circ}\text{C}$ prior to ion formation (13+ – 6+).⁵¹ In both of these chemical¹⁷ and thermal⁵¹ denaturation experiments, the observation of a bimodal CSD at intermediate denaturing conditions was attributed to a two-state unfolding process,^{52,53} where the high-charge and low-charge ions are formed by ionization of the populations of unfolded and folded proteins, respectively.

Assuming a two-state model, the population of unfolded conformers here is determined from the sum of the relative abundances of the 17+ – 7+ ions, and the population of folded conformers from the sum of the relative abundances of the 6+ – 4+ ions. The fraction of unfolded ubiquitin as a function of nESI spray potential at four different entrance capillary temperatures is shown in Figure 1d. At the lowest and highest capillary entrance temperatures (150 and 300 $^{\circ}\text{C}$, respectively), the spray potential has little effect on the extent of unfolded structures. In contrast, the abundance of unfolded structures depends strongly on

the spray potential at intermediate temperatures. For all source temperatures above 150 °C, the total ion abundance is typically greater at the higher spray potentials.

To determine if the transition from folded to unfolded structures with a change in spray potential is reversible, equine cytochrome *c* was continuously nanoelectrosprayed while the spray potential was switched 20 times between 0.8 and 1.8 kV. Similar to the results for ubiquitin shown in Figure 1b, cytochrome *c* nanoelectrosprayed at 1.8 kV (entrance capillary at 200 °C) results in a bimodal CSD (Figure 2), consistent with previous results from heated solutions.^{51,54} For the 10 spectra obtained at 1.8 kV, the average fraction unfolded (0.79 ± 0.03) is significantly higher than that obtained at 0.8 kV (0.06 ± 0.03). The total ion abundance at the 1.8 kV spray potential was, on average, $\sim 4\times$ higher than at 0.8 kV. After alternating the spray potential 20 times, it was not possible to maintain a stable spray at 1.8 kV, but spectra obtained at sufficient spray potential to obtain high-charge ions with high relative abundance could be maintained for more than five minutes. These results demonstrate that it is possible to rapidly switch between a low-charge, native distribution of ions and a high-charge, unfolded distribution of ions, and to maintain a sufficiently high spray potential long enough to obtain both MS and MS/MS data of high charge, unfolded protein ions.

Effects of Different ESI Interfaces on Electrothermal Supercharging

The normal operating temperature range and hardware geometries of ion sources vary from instrument to instrument. To determine if this electrothermal supercharging method could be duplicated on different ion sources that are operated at lower temperatures, spectra of a mixture of cytochrome *c* and ubiquitin (100 mM ammonium bicarbonate, pH 7.3 aqueous solution) were obtained on the 9.4 T Berkeley-Bruker FT-ICR⁴⁶ with the entrance capillary set to either 125 or 180 °C (the maximum operating temperature). A bimodal charge-state distribution was observed at the highest temperature/spray potentials for both proteins, similar to the results obtained on the Thermo LTQ instrument. The fraction unfolded calculated from the relative abundances (corrected for ion charge) of the high-charge ions (ubq: 14+ – 7+; cyt *c*: 16+ – 9+) and low-charge ions (ubq: 6+ – 5+; cyt *c*: 8+ – 7+) as a function of nESI spray potential are shown in Figure 3. No high-charge ions are observed for either protein at 125 °C, even at the highest spray potentials where stable nESI can be reliably maintained (1.4 kV). In contrast, the population of high-charge ions increased significantly with increasing spray potential for cytochrome *c* at 180 °C. The fraction of unfolded ubiquitin also increases with increasing spray potential at the highest entrance capillary temperature, but to a lesser extent than that observed for cytochrome *c*. Within this range of spray potentials, the total ion abundance did not vary by more than 30%.

Similar experiments were performed on a Waters Q-TOF Premier instrument, which is equipped with a “z-spray” ion source that utilizes a skimmer cone with a small aperture to separate atmospheric pressure from the first pumping stage of the instrument. This source is normally operated at ~ 80 °C, but was increased to 140 °C for this experiment. No high-charge ions for either protein could be formed even up to ~ 2 kV spray potential. In addition to the lower operating temperature, the “z-spray” source geometry may play a role in keeping the proteins in their native conformations in solution throughout the ESI introduction process.

Effects of Ionic Strength and Buffer Identity on Protein Charge-state Distributions

Previous supercharging experiments with *m*-NBA in ammonium acetate solutions showed a decrease in the extent of supercharging with an increase in the ionic strength of the solution, consistent with more stable protein structure at higher ionic strength.³² Both the ammonium cation and acetate anion fall on the ‘stabilizing’ ends of the respective Hofmeister series.⁵⁵

To determine the effects of ionic strength on electrothermal supercharging, nESI mass spectra from solutions of 10 μ M ubiquitin in pure water and up to 1.0 M ammonium bicarbonate, pH 7.0, were measured over a range of spray potentials between 0.75 and 1.3 kV. In contrast to supercharging with *m*-NBA in ammonium acetate, the extent of electrothermal supercharging with ammonium bicarbonate is higher at 100 mM (Figure 4), where the effect appears maximized at the source temperature used (220 °C), than at 1 or 10 mM. With 0.5 and 1.0 M ammonium bicarbonate, the highest spray potential tested (1.3 kV) is required to approach the fraction unfolded observed with 100 mM between 0.9 and 1.3 kV (\sim 0.78). At lower spray potentials, the extent of unfolding is significantly lower in the 500 mM and 1 M bicarbonate solutions. As was the case for the mixture of ubiquitin and cytochrome *c*, the total ion abundance did not vary by more than 30% over this range of spray potentials. The fraction unfolded in the pure water solution is \sim 0.13 and does not vary as a function of the spray potential. In contrast, the fraction unfolded in the 1 mM solution is $<$ 0.10 at the lower spray potentials (0.75 – 1.10 kV). This difference may be due to the folded form of the protein being stabilized at low ammonium bicarbonate concentration, but the results at higher concentration suggest that the ammonium bicarbonate contributes to protein unfolding in the ESI droplets.

In striking contrast to the results obtained with ammonium bicarbonate, high charge-state ions of proteins could not be obtained using this method when 100 mM ammonium acetate was used as a buffer. To determine if the difference in electrothermal supercharging between bicarbonate and acetate is, in part, related to Hofmeister stabilization/destabilization effects^{55,56} in the ESI droplets, four other ammonium salts that span the range of the Hofmeister anion series were used as “buffers” in 10 mM, pH 7.0, solutions containing 20 μ M ubiquitin. The ordering of the effectiveness of the different ammonium salts for inducing protein denaturation (fraction unfolded) obtained here: phosphate (0.98 ± 0.01) $>$ thiocyanate (0.95 ± 0.01) $>$ bicarbonate (0.7 ± 0.2) $>$ sulfate (0.6 ± 0.5) $>$ perchlorate (no high-charge ions) \sim acetate (no high-charge ions) does not follow the expected ordering. Phosphate is on the stabilizing end of the Hofmeister series and perchlorate is on the destabilizing end of the series.⁵⁵ Here, their effects are the opposite. Using these results for fraction unfolded, we also examined their relative solution- and gas-phase acidities, solvation energies, and solubilities, but none of these physical parameters correlate with the extent of supercharging observed without at least one significant outlier for a given parameter. These trends are under further investigation. Although phosphate and thiocyanate appear to induce more efficient unfolding under these conditions, bicarbonate is a superior choice for electrothermal supercharging because there is no competing cluster ions formed or ion adduction with ammonium bicarbonate, and the overall signal-to-noise ratios are better.

Mechanism of Electrothermal Supercharging

Proteins can unfold in solution as a result of many factors, including changes in pH or temperature. For positive ions, ESI solutions become more acidic with time,^{57,58} and protein conformational changes induced by ‘pulsating’ versus ‘cone-jet’ mode ESI have been attributed to differences in the solution pH when spraying in these two different regimes.⁵⁹ Here, electrical contact with the solution is made with a platinum wire which is located 5 mm from the tip where droplets are formed. Any pH change that occurs at the electrode surface will take time to diffuse to the tip, and no time dependence to the electrothermal supercharging effect was observed. Furthermore, the supercharging effect is fully reversible with a change in the magnitude of the spray potential, indicating that the pH of the bulk solution is not changing sufficiently to induce structural changes. In addition, the extent of supercharging increases with increasing buffer capacity of the ammonium bicarbonate up to 100 mM, which is inconsistent with any pH change in the bulk solution or ESI droplet.

Thermal denaturation of proteins is well known, but even with the capillary entrance temperature of 300 °C on the Thermo LTQ, the air temperature inside the ESI source is just 40 °C, which is significantly less than the >100 °C temperature required to unfold ubiquitin in neutral pH, aqueous solutions.^{52,53} Thermal unfolding of cytochrome *c* at neutral pH occurs in two steps, with a minor transition at ~50 °C and then a major one at ~85 °C.^{60–62} These significantly higher equilibrium unfolding temperatures strongly suggest that the bimodal charge-state distributions observed in these experiments are the result of rapid thermal denaturation of the protein analytes *in the ESI droplets*, because the nESI emitter is at too low of a temperature for unfolding to occur in bulk solution and unfolding after a bare ion is formed cannot result in increased ion charging. Droplet heating appears to occur through increasingly energetic collisions with gaseous molecules between the nESI emitter tip and the heated entrance capillary when the nESI spray voltage is increased, as well as through collisions with hot neutral gas molecules (and blackbody radiation) within the entrance capillary. The nESI spray potential can also affect the spray characteristics, which may also play a role. Similar enhanced charging is observed when the source region is purged with SF₆ gas, indicating that an electrical discharge does not play a role in electrothermal supercharging, although some fragmentation of the higher charge state ions was observed, presumably due to the high center-of-mass collision energy. Aqueous ammonium bicarbonate decomposes to ammonia, carbon dioxide and water at elevated solution temperature, but the rate of decomposition is much too slow to significantly affect the buffer composition during the ESI droplet lifetime.⁶³

The significant increase in the fraction of unfolded protein with increasing spray potential observed at 175 and 200 °C for ubiquitin (Figure 1d), and for cytochrome *c* at 200 °C (Figure 2), indicates that the effective temperatures of the ESI droplets may be controlled by increasing or decreasing the droplet acceleration. Similar control over the effective temperature of the droplets is evident from the results obtained from the mixture of ubiquitin and cytochrome *c* (Figure 3, data at 180 °C). The significantly higher extent of electrothermal supercharging of cytochrome *c* compared to ubiquitin in the mixture is consistent with thermal unfolding, because the melting temperatures of cytochrome *c* (50 and 85 °C)^{60–62} are lower than that of ubiquitin (> 100 °C),^{52,53} although other factors, such as the rates of unfolding, will contribute to the observed fraction unfolded.

The precision of the ubiquitin data at the intermediate temperatures is lower than it is for the data at the temperature extremes, as indicated by the larger error bars on the 175 and 200 °C data compared to the 150 and 300 °C data in Figure 1d. This is consistent with the thermal unfolding behavior of ubiquitin, where the transition from predominantly folded to predominantly unfolded conformations occurs in a narrow (~10 °C at pH 3.6) temperature range,⁵¹ so that small variations in solution temperature can result in significant changes to the relative populations of folded and unfolded analyte molecules. Here, small variations in the collisional energy deposition into the ESI droplets would produce small changes in droplet temperatures that would result in large changes in the relative populations of unfolded and folded conformers causing the observed decrease in precision at the intermediate temperatures where the transition between these forms of the protein occurs.

Protein denaturation/destabilization in ESI droplets is the principle origin of the formation of highly charged ions with aqueous solution supercharging using reagents, such as *m*-NBA.^{29–34} Protein unfolding in ESI droplets has also been induced by McLuckey and co-workers who entrained vapors of acidic⁶⁴ and basic⁶⁵ molecules into the counter-current drying gas in the atmosphere/vacuum interface to cause pH-induced protein unfolding in ESI droplets formed from unbuffered solutions. Interestingly, the two-state unfolding observed here for ubiquitin was not observed previously in aqueous solution supercharging experiments using 1% *m*-NBA.³³ This may be due to a distribution of *m*-NBA

concentrations in the evaporating droplets. In addition, the extent of supercharging of ubiquitin with 1% *m*-NBA is significantly lower (maximum 10+ ion) than that obtained here with electrothermal supercharging (maximum 17+ ion), suggesting that the protein unfolding induced here by droplet heating is far more extensive and efficient than that which can be achieved through chemical/thermal means^{29–34} using supercharging reagents. Furthermore, in the absence of conformational changes, supercharging reagents in purely aqueous solutions can reduce ion charge because of lowered droplet surface tension, mitigating the extent of supercharging.^{22,30} These results clearly demonstrate that for instruments with “hot” ion sources, such as the Thermo LTQ equipped with a heated metal entrance capillary, electrothermal supercharging is more effective than supercharging reagents at forming high-charge protein ions from purely aqueous solutions.

The effects of entrance capillary temperature on protein unfolding using other solvent systems have been examined. For example, Mirza and Chait found no significant unfolding as a function of capillary entrance temperature (up to 300 °C) for ubiquitin in aqueous acetic acid (pH 2.4) or 70:30 water:methanol, lysozyme in aqueous acetic acid (pH 2.9) or 50:50 water:methanol, or cytochrome *c* in 50:50 water:methanol.⁶⁶ In contrast, they did observe modest unfolding of lysozyme in 50:50 water:methanol containing 5 mM ammonium acetate, cytochrome *c* in 50:50 water:methanol containing 10 mM ammonium acetate, and myoglobin in 70:30 water:methanol containing 10 mM ammonium acetate. The authors hypothesized that the presence of the ammonium acetate may extend the ESI droplet lifetimes, enabling higher energy deposition through collisions with neutrals and concomitant droplet/analyte heating.⁶⁶ Results from an elegant experiment that replaced dry nitrogen with humid nitrogen in the atmosphere/vacuum interface of their ESI source were consistent with this hypothesis. A similar effect may account for the enhanced supercharging observed here from ammonium bicarbonate solutions compared to pure aqueous solutions. Dixon and coworkers have also examined the effect of entrance capillary temperature on protein CSDs.⁶⁷ Using a 13.6 kDa truncation mutant of the protein DnaB from *Escherichia coli* in a 10 mM ammonium acetate, pH 7.6, solution, they observed no significant change in the charge-state distribution when the entrance capillary temperature was increased from 40 to 240 °C for positive ion ESI.⁶⁷ Interestingly, a significant increase in the fraction unfolded was observed for negative ion ESI of the same protein when the entrance capillary temperature was increased from 40 to 240 °C. In all of these previously reported examples where unfolding is induced with droplet heating, the proteins were either destabilized chemically prior to ESI⁶⁶ or had populations of unfolded protein even when the entrance capillary temperature was just 40 °C,⁶⁷ indicating that the folded forms of the proteins were only marginally stable in the initial solutions. Laserspray ionization has also been used to rapidly denature proteins from fully aqueous buffered solutions at neutral pH.⁶⁸

Conclusions

Electrothermal supercharging makes possible the reversible formation of narrow, low-charge distributions and broad, high-charge distributions of protein ions formed by nESI from purely aqueous, ammonium bicarbonate solutions at neutral pH simply by changing the nESI spray potentials. The primary origin of the high-charge ions appears to be denaturation induced by rapid heating of the ESI droplet that occurs in the atmosphere/vacuum interface and is enhanced by a destabilizing effect caused by the bicarbonate anion. For instruments with energetic ESI interfaces, the extent of supercharging is much greater than has been achieved with supercharging reagents, such as *m*-NBA or sulfolane. In contrast, supercharging reagents are more effective for “cool” ion sources, such as the Waters “z-spray” source.^{29,31,32} The capability to rapidly and reversibly switch from “native” ESI to effectively denaturing ESI from the same buffered aqueous solution with only a change in the ESI potential could be advantageous for analytical measurements. For example, it may

be desirable to monitor a change in the native, solution-phase structure by measuring subtle shifts in the ESI charge-state distribution³ or measuring ion mobility arrival time distributions under native conditions, and then rapidly switch to a high-charge distribution to obtain MS/MS spectra with much higher fragmentation efficiency and sequence coverage than is possible with lower charge-state ions. Another application is an extension of real-time HDX-MS³³ to larger and/or more stable analytes that are not sufficiently charged with supercharging reagents. At a minimum, electrothermal supercharging should obviate the need for organic solvents and acids in nESI solutions so that large proteins can be ionized from buffered, neutral pH, solution conditions and analyzed with mass spectrometers with limited m/z range. This technique may also find application in the development of new ion sources as a means to measure relative droplet temperatures during the ESI process. Although this reversible electrothermal supercharging method was demonstrated with nESI, high charge state ubiquitin ions are also formed from aqueous ammonium bicarbonate solutions using a standard ESI interface with a solution flow rate of 5 $\mu\text{L}/\text{min}$ at high source temperature, suggesting that this method to produce high charge state ions should be broadly applicable. Finally, these results suggest that ~ 150 mM ammonium bicarbonate may be the ideal buffer for nESI of native proteins because the electrothermal supercharging effect can be controlled and maximized, there are no adverse effects on total ion abundance, the solution will be adequately buffered at pH ~ 7 , and 150 mM ammonium bicarbonate has an ionic strength that is similar to that of many biological samples.

Supplementary Material

Refer to Web version on PubMed Central for supplementary material.

Acknowledgments

The authors thank the National Institutes of Health (grant no. R01GM096097 and training grant T32GM008295 for H.J.S.) for generous financial support and Tawnya G. Flick for helpful discussion.

References

1. Heck AJR. *Nature Methods*. 2008; 5:927–933. [PubMed: 18974734]
2. Rostom AA, Tame JRH, Ladbury JE, Robinson CV. *J. Mol. Biol.* 2000; 296:269–279. [PubMed: 10656831]
3. Kintzer AF, Sterling HJ, Tang II, Abdul-Gader A, Miles AJ, Wallace BA, Williams ER, Krantz BA. *J. Mol. Biol.* 2010; 399:741–758. [PubMed: 20433851]
4. Hernandez H, Hewitson KS, Roach P, Shaw NM, Baldwin JE, Robinson CV. *Anal. Chem.* 2001; 73:4154–4161. [PubMed: 11569804]
5. Lorenzen K, Olia AS, Uetrecht C, Cingolani G, Heck AJR. *J. Mol. Biol.* 2008; 379:385–396. [PubMed: 18448123]
6. Batchelor JD, Sterling HJ, Hong E, Williams ER, Wemmer DE. *J. Mol. Biol.* 2009; 393:634–643. [PubMed: 19699748]
7. Kintzer AF, Thoren KL, Sterling HJ, Dong KC, Feld GK, Tang II, Zhang TT, Williams ER, Berger JM, Krantz BA. *Journal of Molecular Biology.* 2009; 392:614–629. [PubMed: 19627991]
8. Painter AJ, Jaya N, Basha E, Vierling E, Robinson CV, Benesch JLP. *Chem. Biol.* 2008; 15:246–253. [PubMed: 18355724]
9. Uetrecht C, Watts NR, Stahl SJ, Wingfield PT, Steven AC, Heck AJR. *Phys. Chem. Chem. Phys.* 2010; 12:13368–13371. [PubMed: 20676421]
10. Breuker K, Oh HB, Horn DM, Cerda BA, McLafferty FW. *J. Am. Chem. Soc.* 2002; 124:6407–6420. [PubMed: 12033872]
11. Iavarone AT, Williams ER. *Anal. Chem.* 2003; 75:4525–4533. [PubMed: 14632060]
12. Madsen JA, Brodbelt JS. *J. Am. Soc. Mass Spectrom.* 2009; 20:349–358. [PubMed: 19036605]

13. Zubarev RA, Kelleher NL, McLafferty FW. *J. Am. Chem. Soc.* 1998; 120:3265–3266.
14. Iavarone AT, Paech K, Williams ER. *Anal. Chem.* 2004; 76:2231–2238. [PubMed: 15080732]
15. Marshall AG, Hendrickson CL, Jackson GS. *Mass Spectrom. Rev.* 1998; 17:1–35. [PubMed: 9768511]
16. Chowdhury SK, Katta V, Chait BT. *J. Am. Chem. Soc.* 1990; 112:9012–9013.
17. Loo JA, Loo RRO, Udseth HR, Edmonds CG, Smith RD. *Rapid Comm. Mass Spectrom.* 1991; 5:101–105.
18. Kebarle P, Verkerk UH. *Mass Spectrom. Rev.* 2009; 28:898–917. [PubMed: 19551695]
19. Dobo A, Kaltashov IA. *Anal. Chem.* 2001; 73:4763–4773. [PubMed: 11681449]
20. Iavarone AT, Jurchen JC, Williams ER. *Anal. Chem.* 2001; 73:1455–1460. [PubMed: 11321294]
21. Iavarone AT, Williams ER. *Int. J. Mass Spectrom.* 2002; 219:63–72.
22. Iavarone AT, Williams ER. *J. Am. Chem. Soc.* 2003; 125:2319–2327. [PubMed: 12590562]
23. Sze SK, Ge Y, Oh H, McLafferty FW. *Proc. Natl. Acad. Sci. U. S. A.* 2002; 99:1774–1779. [PubMed: 11842225]
24. Davies NW, Wiese MD, Browne SGA. *Toxicol.* 2004; 43:173–183. [PubMed: 15019477]
25. Kjeldsen F, Giessing AMB, Ingrell CR, Jensen ON. *Anal. Chem.* 2007; 79:9243–9252. [PubMed: 18020370]
26. Valeja SG, Tipton JD, Emmett MR, Marshall AG. *Anal. Chem.* 2010; 82:7515–7519. [PubMed: 20704305]
27. Lomeli SH, Yin S, Loo RRO, Loo JA. *J. Am. Soc. Mass Spectrom.* 2009; 20:593–596. [PubMed: 19101165]
28. Lomeli SH, Peng IX, Yin S, Loo RRO, Loo JA. *J. Am. Soc. Mass Spectrom.* 2010; 21:127–131. [PubMed: 19854660]
29. Sterling HJ, Williams ER. *J. Am. Soc. Mass Spectrom.* 2009; 20:1933–1943. [PubMed: 19682923]
30. Sterling HJ, Cassou CA, Trnka MJ, Burlingame AL, Krantz BA, Williams ER. *Phys. Chem. Chem. Phys.* 2011; 13:18288–18296. [PubMed: 21399817]
31. Sterling HJ, Daly MP, Feld GK, Thoren KL, Kintzer AF, Krantz BA, Williams ER. *J. Am. Soc. Mass Spectrom.* 2010; 21:1762–1774. [PubMed: 20673639]
32. Sterling HJ, Kintzer AF, Feld GK, Cassou CA, Krantz BA, Williams ER. *J. Am. Soc. Mass Spectrom.* 2012; 23:191–200. [PubMed: 22161509]
33. Sterling HJ, Williams ER. *Anal. Chem.* 2010; 82:9050–9057.
34. Sterling HJ, Prell JS, Cassou CA, Williams ER. *J. Am. Soc. Mass Spectrom.* 2011; 22:1178–1186. [PubMed: 21953100]
35. Hogan CJ, Loo RRO, Loo JA, de la Mora JF. *Phys. Chem. Chem. Phys.* 2010; 12:13476–13483. [PubMed: 20877871]
36. Erba EB, Ruotolo BT, Barsky D, Robinson CV. *Anal. Chem.* 2010; 82:9702–9710. [PubMed: 21053918]
37. Regazzoni L, Bertolotti L, Vistoli G, Colombo R, Aldini G, Serra M, Carini M, Caccialanza G, De Lorenzi E. *ChemMedChem.* 2010; 5:1015–1025. [PubMed: 20544784]
38. Yin S, Loo JA. *Int. J. Mass Spectrom.* 2011; 300:118–122. [PubMed: 21499519]
39. Enyenihi AA, Yang H, Ytterberg AJ, Lyutvinskiy Y, Zubarev RA. *J. Am. Soc. Mass Spectrom.* 2011; 22:1763–1770. [PubMed: 21952890]
40. Grimm RL, Beauchamp JL. *J. Phys. Chem. A.* 2010; 114:1411–1419. [PubMed: 19848399]
41. Samalikova M, Grandori R. *J. Am. Chem. Soc.* 2003; 125:13352–13353. [PubMed: 14583019]
42. Douglass KA, Venter AR. *J. Am. Soc. Mass Spectrom.* 2012 10.1007/s13361-13011-10319-13361.
43. Kebarle P, Tang L. *Anal. Chem.* 1993; 65:972–986.
44. Valeja SG, Kaiser NK, Xian F, Hendrickson CL, Rouse JC, Marshall AG. *Anal. Chem.* 2011; 83:8391–8395. [PubMed: 22011246]
45. Compton PD, Zamdborg L, Thomas PM, Kelleher NL. *Anal. Chem.* 2011; 83:6868–6874. [PubMed: 21744800]
46. Jurchen JC, Williams ER. *J. Am. Chem. Soc.* 2003; 125:2817–2826. [PubMed: 12603172]

47. Verkerk UH, Peschke M, Kebarle P. *J. Mass Spectrom.* 2003; 38:618–631. [PubMed: 12827631]
48. Iavarone AT, Udekwu OA, Williams ER. *Anal. Chem.* 2004; 76:3944–3950. [PubMed: 15253628]
49. Yang PX, Cooks RG, Ouyang Z, Hawkridge AM, Muddiman DC. *Anal. Chem.* 2005; 77:6174–6183. [PubMed: 16194076]
50. Babu KR, Moradian A, Douglas DJ. *J. Am. Soc. Mass Spectrom.* 2001; 12:317–328. [PubMed: 11281607]
51. Mirza UA, Cohen SL, Chait BT. *Anal. Chem.* 1993; 65:1–6. [PubMed: 8380538]
52. Wintrode PL, Makhatadze GI, Privalov PL. *Proteins Struct. Funct. Gen.* 1994; 18:246–253.
53. Makhatadze GI, Lopez MM, Richardson JM, Thomas ST. *Prot. Sci.* 1998; 7:689–697.
54. Le Blanc JCY, Beuchemin D, Siu KWM, Guevremont R, Berman SS. *Org. Mass Spectrom.* 1991; 26:831–839.
55. Collins KD, Washabaugh MW. *Q. Rev. Biophys.* 1985; 18:323–422. [PubMed: 3916340]
56. Cacace MG, Landau EM, Ramsden JJ. *Q. Rev. Biophys.* 1997; 30:241–277. [PubMed: 9394422]
57. Gatlin CL, Turecek F. *Anal. Chem.* 1994; 66:712–718.
58. VanBerkel GJ, Zhou FM, Aronson JT. *Int. J. Mass Spectrom. Ion Proc.* 1997; 162:55–67.
59. Nemes P, Goyal S, Vertes A. *Anal. Chem.* 2008; 80:387–395. [PubMed: 18081323]
60. Bull HB, Breese K. *Arch. Biochem. Biophys.* 1973; 156:604–612. [PubMed: 4352419]
61. Myer YP. *Biochemistry.* 1968; 7:765–776. [PubMed: 5689422]
62. Urry DW. *Proc. Natl. Acad. Sci. U.S.A.* 1965; 54:640–648. [PubMed: 5217450]
63. Nowak P, Skrzypek J. *Chem. Eng. Sci.* 1989; 44:2375–2377.
64. Kharlamova A, Prentice BM, Huang TY, McLuckey SA. *Anal. Chem.* 2010; 82:7422–7429. [PubMed: 20712348]
65. Kharlamova A, McLuckey SA. *Anal. Chem.* 2011; 83:431–437. [PubMed: 21141935]
66. Mirza UA, Chait BT. *Int. J. Mass Spectrom. Ion Proc.* 1997; 162:173–181.
67. Watt SJ, Sheil MM, Beck JL, Prosselkov P, Otting G, Dixon NE. *J. Am. Soc. Mass Spectrom.* 2007; 18:1605–1611. [PubMed: 17629493]
68. Shi XG, Takamizawa A, Nishimura Y, Hiraoka K, Akashi S. *Rapid Comm. Mass Spectrom.* 2008; 22:1430–1436.

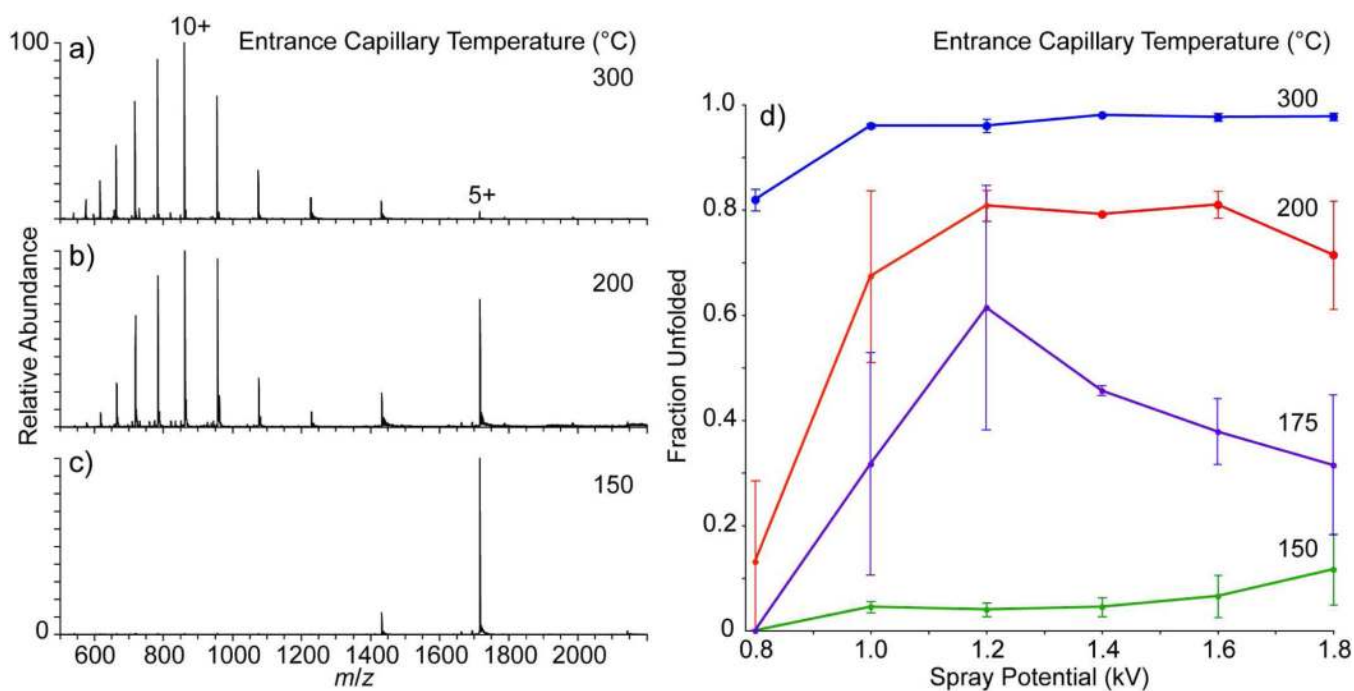


Figure 1. Nanoelectrospray mass spectra of 20 μ M bovine ubiquitin in a 200 mM ammonium bicarbonate, pH 7.0, solution obtained on a Thermo™ LTQ with the entrance capillary temperature set to (a) 300 °C, (b) 200 °C, and (c) 150 °C with a nESI spray potential of 1.2 kV and a spray tip-to-entrance capillary distance of 5 mm. Fraction unfolded as function of nESI spray potential is shown in (d) for four different entrance capillary temperatures.

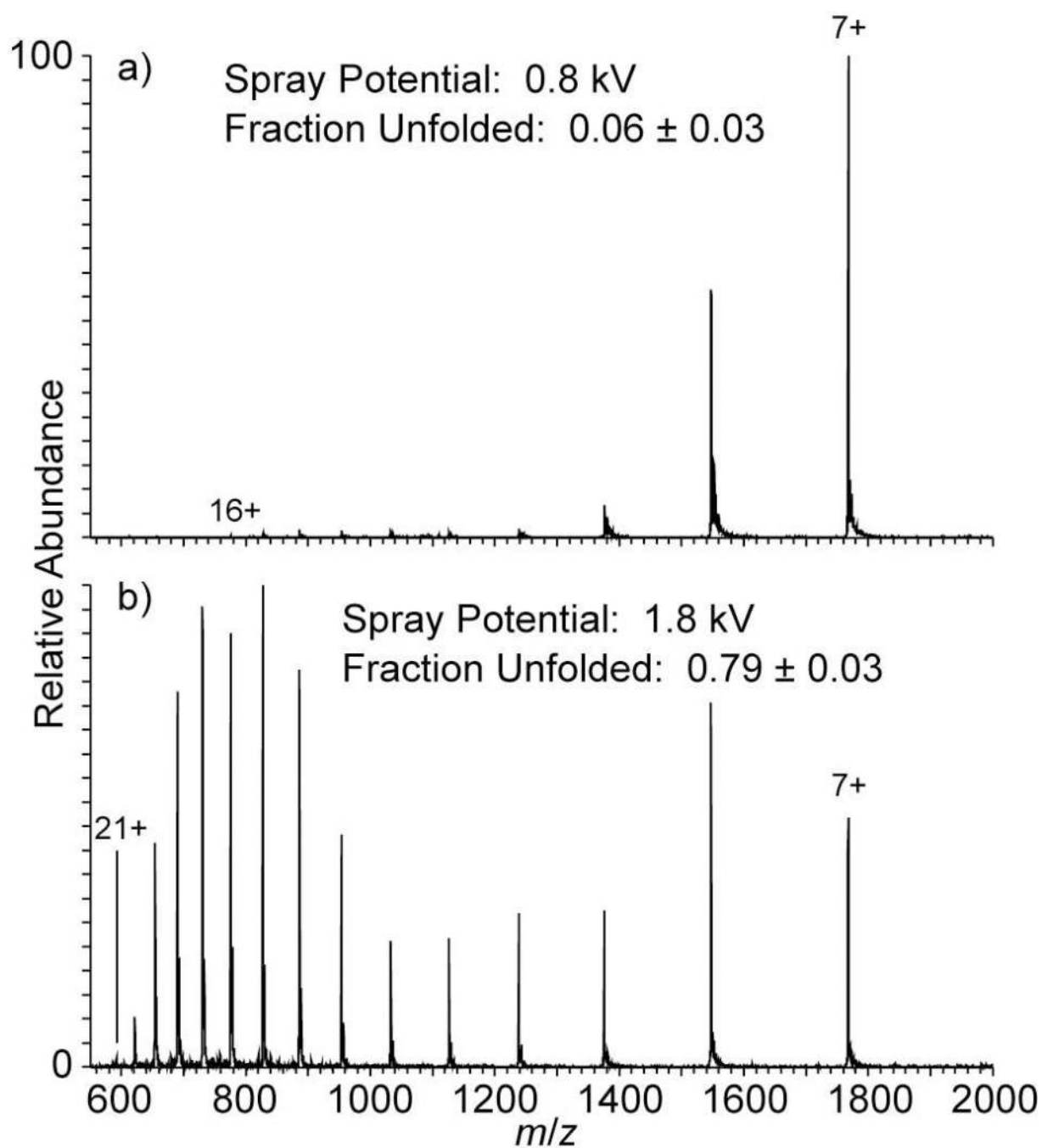


Figure 2. Nanoelectrospray mass spectra of 20 μM equine cytochrome c in a 200 mM ammonium bicarbonate, pH 7.0, solution obtained on a ThermoTM LTQ with the entrance capillary temperature set to 200 $^{\circ}\text{C}$ and the nESI spray potential at either (a) 0.8 kV or (b) 1.8 kV with a spray tip-to-entrance capillary distance of 5 mm. The spray potential was alternated 20 times with 30 s of continuous data obtained after each change in potential.

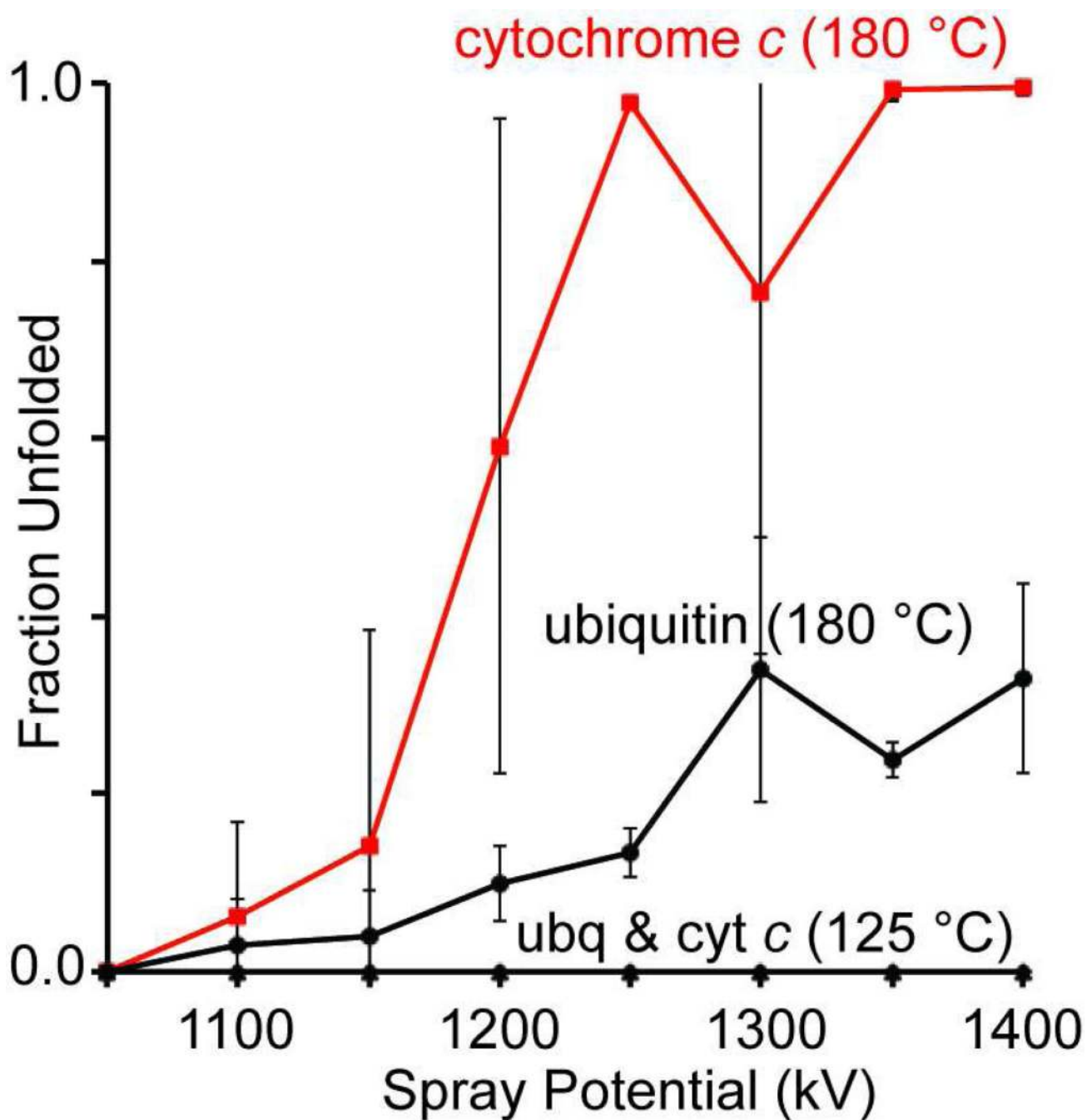


Figure 3. Fraction unfolded as function of nESI spray potential for a mixture of 25 μM cytochrome c and 10 μM ubiquitin in a 100 mM ammonium bicarbonate, pH 7.3, solution with the entrance capillary temperature on the 9.4 T FT-ICR instrument⁴⁶ at either 125 or 180 °C (the maximum temperature). The spray tip-to-entrance capillary distance was 3 mm.

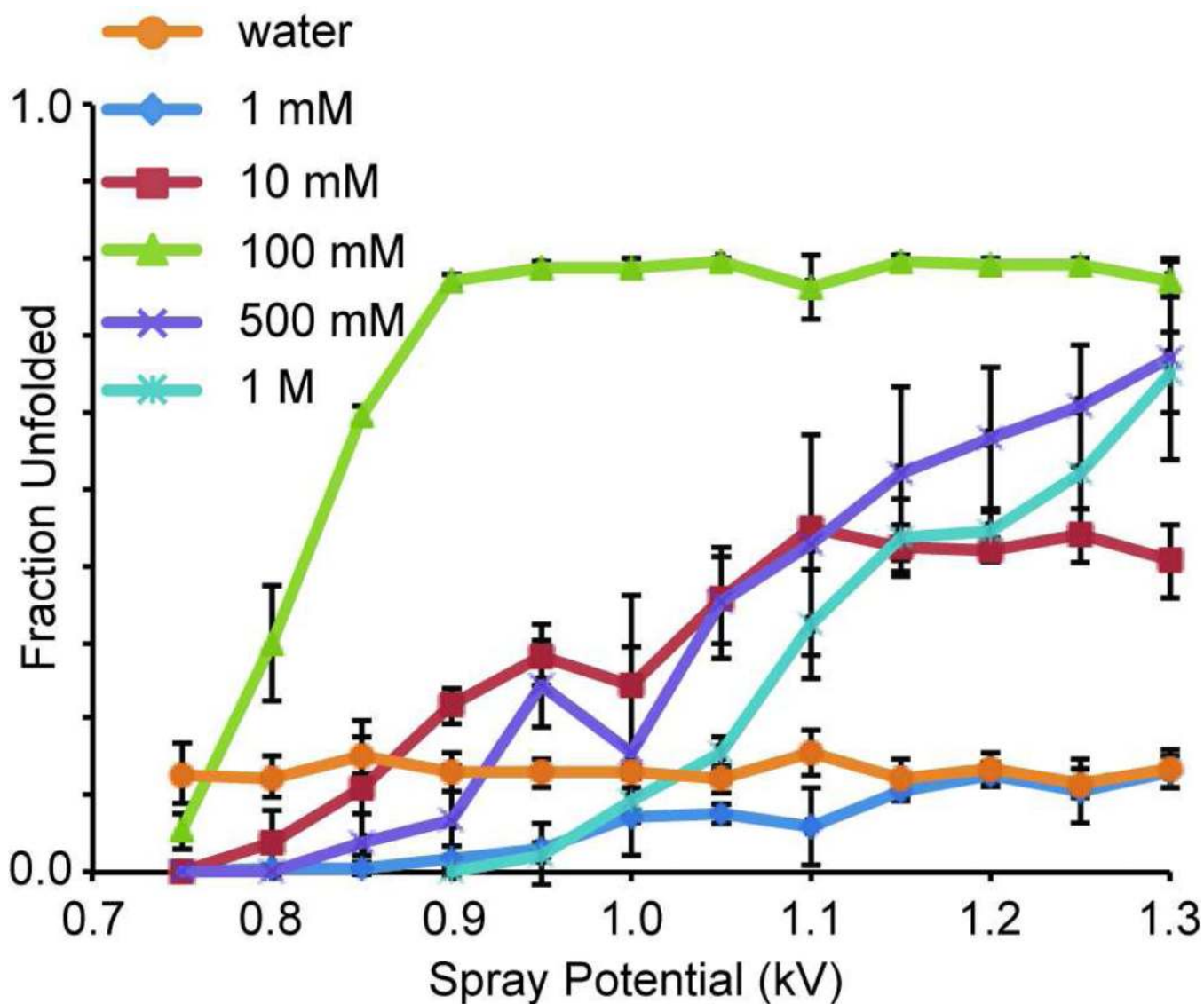


Figure 4. Fraction unfolded as function of nESI spray potential for 10 μ M ubiquitin in either Milli-Q water or pH 7.0 ammonium bicarbonate solutions that vary in concentration from 1 mM to 1 M. The spray tip-to-entrance capillary distance was 5 mm.